Available online at www.sciencedirect.com
SCIENCE DIRECT®
Journal of Power Sources 157 (2006) 78–84
JOURNAL OF POWER SOURCES
www.elsevier.com/locate/jpowsour

Unusually active palladium-based catalysts for the electrooxidation of formic acid

Robert Larsen, Su Ha, Joseph Zakzeski, Richard I. Masel *

Department of Chemical Engineering, University of Illinois at Urbana-Champaign, 600 South Mathews Avenue, Urbana, IL 61801, USA

Received 24 June 2005; received in revised form 19 July 2005; accepted 19 July 2005
Available online 21 October 2005

Abstract

Formic acid fuel cells offer exciting prospects for powering portable electronic and MEMS devices. Pd-based catalysts further improve the performance of direct formic acid fuel cells while reducing catalyst costs over Pt-based catalysts. This study investigates several Pd-based catalysts, both unsupported and carbon-supported, and compares the electrochemical results with results obtained in an operating fuel cell. Power densities of up to 260 mW cm^{-2} were achieved in a fuel cell at 750 mA operating at 30 °C. Carbon-supported catalysts and addition of other metals, such as gold, show potential in further improving the performance of Pd-based catalysts.

Keywords: Palladium-based catalyst; Electrooxidation; Formic acid

1. Introduction

Recently, direct formic acid fuel cells (DFAFCs) have been shown to possess excellent characteristics for powering portable electronic devices and microelectromechanical systems (MEMS) [1,2]. Formic acid is a liquid at room temperature and dilute formic acid is on the US Food and Drug Administration list of food additives that are generally recognized as safe. Formic acid has two orders of magnitude smaller crossover flux through a Nafion® membrane than methanol allowing the use of highly concentrated fuel solutions in DFAFCs [3]. Formic acid also has a higher theoretical electromotive force (EMF) in a fuel cell, as calculated from the Gibbs free energy, than either hydrogen or direct methanol fuel cells (DMFCs). In previous studies, platinum-based catalysts were used on the anode for formic acid oxidation [1,2,4]. *V–I* characteristics of the DFAFC were shown to be dependent upon whether a Pd-doped Pt (Pt/Pd), Ru-doped Pt (Pt/Ru) or a commercial PtRu alloy black were used. The overall activity of platinum-based catalysts was limited due to CO poisoning [2].

It is desirable to develop more active catalysts to improve cell efficiency and power density while reducing overall precious metal loadings. Recently, we have reported on a new class of palladium-based catalysts that boosts the performance of DFAFCs to even better levels than that observed with platinum-based catalysts [5,6]. These new DFAFCs even approach hydrogen fuel cell performances in many cases. It is believed that the lack of CO poisoning on Pd catalysts leads to higher activity than Pt-based catalysts. Limited studies of palladium-based catalysts have been done in the past, but none have utilized Pd catalysts in a fuel cell [7,8]. This study attempts to investigate several different types of Pd-based catalysts both at a fundamental level in an electrochemical cell and in an operating fuel cell.

2. Experimental

The catalysts tested were two Pd blacks (20 $m^2\,g^{-1}$ from Alfa Aesar, 50 $m^2\,g^{-1}$ from Sigma–Aldrich) and three carbon-supported catalysts, 20 wt% Pd on Vulcan XC-72 carbon, 40 wt% Pd on Vulcan XC-72 carbon and 20 wt% PdAu (50 atoms Pd:1 atom Au ratio) on Vulcan XC-72 carbon prepared in house.

The carbon-supported catalysts were prepared by a metal chloride reduction process. First, the Vulcan XC-72 carbon was conditioned according to Biella et al. [9], by stirring in 10 M

* Corresponding author. Tel.: +1 217 333 3640; fax: +1 217 333 5052.
E-mail address: r-masel@uiuc.edu (R.I. Masel).

0378-7753/$ – see front matter © 2005 Elsevier B.V. All rights reserved.
doi:10.1016/j.jpowsour.2005.07.066

HCl in Millipore water for 12 h and then rinsing with Millipore water until the pH reached 7. Next, a certain volume of a 8 g L^{-1} $PdCl_2$ solution in 5 M HCl and Millipore water was added to a beaker depending on the desired wt% of Pd:

(1) for the 20 wt% Pd and Pd Au on carbon, 5 mL of solution was added;
(2) for the 40 wt% Pd on carbon, 14 mL of solution was added.

One millilitre of a 5 g L^{-1} polyvinyl alcohol (PVA) in Millipore water solution was also added to the beaker. Hundred milligrams of carbon was then added along with enough water to make 1 L total. The solution was then stirred vigorously while 50 mL of freshly prepared 0.05 M $NaBH_4$ in Millipore water was added drop-wise. When this was done, the pH of the solution was raised to ~11 by addition of 5 M NaOH. The solution was then stirred vigorously for 1 h, after which the catalyst was allowed to settle for an additional 30 min. The carbon-supported catalyst was then filtered, rinsed in Millipore water and dried at 80 °C for 8 h.

For the PdAu alloy on carbon (50 Pd:1 Au ratio on an atom basis), a $HAuCl_4$ solution was prepared by dissolving the desired amount of gold powder (Alfa Aesar) in a minimum amount of aqua regia (3 parts concentrated HCl to 1 part concentrated HNO_3 by volume) and removing the HNO_3 by heating. This was then added to the solution at the same stage as the $PdCl_2$ addition following the same procedures as above.

Active metal surface area of the two palladium blacks and three supported catalysts were determined by CO chemisorption measurements. A sample of the catalyst to be measured was first weighed and then prepared. All steps were performed at room temperature. First, a 30% H_2/70% He mixture at 20 sccm was flowed over the catalyst for 2 h. Next, pure H_2 at 20 sccm was flowed over the catalyst. Then, an inert He atmosphere was introduced at 20 sccm. The 50.1 μL pulses of CO were introduced until the catalyst surface became saturated and the total adsorbed CO was determined. The active metal surface area was then calculated assuming on top adsorption (1 CO molecule/atom of Pd).

Electrochemical measurements were taken using a Solartron SI 1287 attached to a PC using the CorrWare software. All experiments were performed at room temperature in air using a custom designed three-electrode cell. The counter electrode was made from a 25 mm × 50 mm piece of 52 mesh platinized platinum gauze (woven from 0.1 mm diameter wire, 99.9%, Alfa Aesar) attached to a platinum wire (0.6 mm diameter, 12 cm long, 99.95%, Alfa Aesar). The reference electrode was Ag/AgCl in 3.0 M NaCl (BAS, MF-2052). However, all results are reported versus the reversible hydrogen electrode (RHE).

All four catalysts were attached to a graphite working electrode for testing in the electrochemical cell. First, 5 mg mL^{-1} suspensions of each of the catalysts in Millipore water were made. Then, enough of a 5 wt% Nafion solution (1100 EW, Solution Technologies Inc.) was added to give a 20 wt% Nafion in the catalyst layer when dried. Each catalyst was sonicated for 10 min. Next, 50 μL of the suspension was placed on the graphite working electrode using a micropipette and dried under a heat lamp for ~25 min. After drying, the electrode was allowed to cool for ~10 min and then rinsed with Millipore water. All working electrodes were stable and no catalyst particles were observed to detach during the experiments.

Catalyst samples were tested in the custom three-electrode cell by contact of the working electrode with the interface of a 5 M HCOOH/0.1 M H_2SO_4 solution (from 88% ACS grade formic acid and 96% double distilled sulfuric acid, GFS Chemicals) contained within the cell. Chronoamperometry was then performed by holding the working electrode at 0.3 V versus the reversible hydrogen electrode while measuring the current over time.

CO stripping voltammetry was performed on Johnson-Matthey platinum black and Sigma–Aldrich high surface area palladium black. In these experiments, oxidation of 5 M HPLC grade formic acid (Fluka) in 0.5 M H_2SO_4 (GFS) was run for 1 h at 0.3 V (RHE). Then, the cell was flushed with 0.1 M H_2SO_4 and cyclic voltammetry (CV) was run at 10 mV s^{-1}. Only part of the CV, the CO stripping region, is shown.

Membrane electrode assemblies (MEAs) with a 5 cm^2 geometrical active cell area were fabricated using a 'direct paint' technique to apply the catalyst layer. The catalyst inks were prepared by dispersing the catalyst nanoparticles into appropriate amounts of Millipore water and a 5 wt% recast Nafion® solution (1100 EW, Solution Technology Inc.). Anode and cathode catalyst inks were directly painted onto either side of a Nafion® 112 membrane. For all MEAs prepared in this study, the cathode consisted of unsupported platinum black nanoparticles (27 m^2 g^{-1}, Johnson-Matthey) at a standard loading of 8 mg cm^{-2}. The anode consisted of catalyst particles at the following loadings: 2.4 mg cm^{-2} for both commercial Pd blacks, 2.4 mg Pd cm^{-2} for the 40 wt% Pd on carbon (6 mg total cm^{-2}), 1.2 mg Pd cm^{-2} for the 20 wt% Pd on carbon and the 20 wt% PdAu on carbon (6 mg total cm^{-2}). A carbon cloth diffusion layer (E-TeK) was placed on top of both the cathode and anode catalyst layers. Both sides of the cathode side carbon cloth were Teflon® coated for water management. A single cell test fixture consisted of machined graphite flow fields with direct liquid feeds and gold plated copper plates to avoid corrosion (Fuel Cell Technologies Inc.).

The MEAs were initially conditioned within the test fixture at 60 °C under H_2/air fuel cell operating mode for 2 h, while holding the cell potential at 0.6 V. Cell potential was controlled by a fuel cell testing station (Fuel Cell Technologies Inc.). H_2 flow rate was set to 200 sccm, the gas stream was humidified at 70 °C prior to entering the cell and a backpressure of 20 psi was applied. Air flow rate to the cathode was 390 sccm, the gas stream was humidified to 70 °C and a backpressure of 20 psi was applied.

Both upward and downward voltage scans were applied for each cell polarization measurement at 30 °C. The plots in the two scan directions were averaged and presented in this paper as a single curve. On the cathode, dry air was supplied at a flow rate of 390 sccm without any backpressure, while on the anode, 5 M formic acid was fed at 1 mL min^{-1}. Constant voltage tests were performed at a potential difference of 0.39 V and 30 °C for DFAFCs with 5 M formic acid (from 88% ACS grade, GFS

Chemicals) at a flow rate of 1 ml min^{-1}. Again, dry air was supplied at a flow rate of 390 sccm without any backpressure on the cathode.

3. Results

Fig. 1(A–E) shows TEM images of each of the Pd catalysts used. The 20 wt% Pd on carbon contains Pd nanoparticles typically 3–10 nm in size with a few as large as 30 nm. Some of the nanoparticles are agglomerated into clumps with some isolated particles, as well. The PdAu nanoparticles on carbon have roughly the same size but appear to be less agglomerated than the pure Pd nanoparticles on carbon. The Pd nanoparticles present in the 40 wt% Pd on carbon are the roughly the same size, but even more agglomerated than the Pd nanoparticles in the 20 wt% Pd on carbon. The high surface area Pd black from Sigma–Aldrich has a filamentous structure with a high degree of void space. The low surface area Pd black from Alfa Aesar appears to contain large chunks of Pd (>100 nm) with rough surface features.

Table 1 gives the active metal surface areas of the five catalysts as well as the dispersion of the Pd on carbon catalysts as determined by CO chemisorption. The 20 wt% PdAu on carbon has a slightly lower specific active surface area than the 20 wt% Pd on carbon on both a total catalyst weight and Pd weight basis. As expected, the 40 wt% Pd on carbon has a higher surface area on a total catalyst weight basis but a lower surface area on a Pd weight basis. All three carbon catalysts have rather low dispersions (<5%).

Fig. 2(A) shows the chronoamperometric measurements at 0.3 V versus RHE for each of the four catalysts on a total catalyst weight basis while Fig. 2(B) shows activity on a per weight palladium basis. By both measures, the low surface area Pd black from Alfa has the lowest performance and deactivates rather quickly in the first 2 h. The high surface area Aldrich Pd black shows much better performance and deactivates more slowly. Fig. 2(A) demonstrates that the high surface area Aldrich Pd black performs the best overall followed by 40 wt% Pd on carbon, then 20 wt% PdAu on carbon, 20 wt% Pd on carbon and finally, by the low surface area Pd black. When comparing current densities based on Pd content, we see that the deactivation of the Alfa Pd black is substantially greater than the other Pd catalysts. The carbon-supported catalysts show higher current densities than the Aldrich Pd black initially. However, the Aldrich Pd black deactivates more slowly and so, outperforms the carbon-supported catalysts at longer times. The 40 wt% Pd on carbon has a lower initial current density than the two 20 wt% catalysts and deactivates more slowly. From Fig. 2(A and B), it is apparent that the addition of a small amount of gold to the carbon-supported catalyst enhances its performance.

Table 1
Surface area and dispersion data for the Pd catalysts tested

Catalyst	Active metal surface area (m^2 g^{-1} total)	Active metal surface area (m^2 g^{-1} Pd)	Dispersion (%)
Pd black (Aldrich)	50	–	–
Pd black (Alfa)	20	–	–
20 wt% Pd on C	8.0	39.9	4.4
20 wt% PdAu on C	7.8	38.9	4.2
40 wt% Pd on C	13.9	34.8	3.9

Fig. 2(C) compares the chronoamperometric activity of the Pd catalysts at 0.3 V versus RHE on a total surface area basis. The carbon-supported catalysts have the highest initial activity and after 8 h, both the 40 wt% Pd on carbon and the 20 wt% PdAu on carbon perform about the same as the Aldrich Pd black while the 20 wt% Pd on carbon has deactivated further. The low surface area Alfa Pd black has the lowest activity.

Fig. 3(A and B) shows the performance of the Pd anode catalysts in a real fuel cell on both a geometrical active surface area basis and Pd weight basis, respectively. Fig. 3(A) shows that the Alrich Pd black gives the best overall performance, followed by the Alfa Pd black. The 20 wt% PdAu on carbon and the 40 wt% Pd on carbon are next and perform comparably. The 20 wt% Pd on carbon performs slightly lower than the other two carbon-supported catalysts at higher current densities. For all experiments, the fuel cell test is run immediately after activation of the anode catalyst by a pulse at 1.0 V versus DHE, before the low surface area Alfa Pd black has a chance to deactivate. After deactivation, it performs worse than the carbon-supported catalysts. The Alfa Pd black deactivates more rapidly than all other catalysts tested and is therefore a less desirable catalyst. The results in Fig. 3 are therefore consistent with the catalyst activities shown by the chronoamperometric data.

Fig. 3(B) demonstrates the improved use of Pd metal in the low loading carbon-supported catalysts (20 wt% Pd and 20 wt% PdAu on carbon). The unsupported catalysts are somewhat less efficient in using Pd metal, while the 40 wt% Pd on carbon is gives the worst performance on a weight basis.

Fig. 4(A and B) gives the corresponding power density plots for the *V–I* plots in Fig. 3(A and B). Of particular interest in Fig. 3(A), the high surface area Aldrich Pd black shows the highest maximum power density of 260 mW cm^{-2} and is able to provide this at the highest current density of all the catalysts on a geometrical active surface area basis. Fig. 3(B) shows the 20 wt% PdAu catalyst using Pd metal the most efficiently with a power density of 135 mW mg^{-1} at the highest current density on a per Pd catalyst weight basis.

Fig. 5 shows a constant voltage test at 0.39 V in a fuel cell for each of the catalysts used. This corresponds well with the data from Fig. 2. The Alfa Pd black deactivates the most rapidly and the other catalysts have similar deactivation rates. The Aldrich Pd black again performs the best.

We have also looked for CO buildup on Pt and Pd catalysts as a result of formic acid oxidation. Fig. 6 shows the surface buildup of CO after 1 h of oxidation at 0.3 V versus RHE in 5 M HPLC grade formic acid/0.5 M H_2SO_4, Johnson-Matthey platinum black and Sigma–Aldrich high surface area palladium black.

In the case of platinum, there is a large peak at 0.68 V (RHE). This peak is characteristic of oxidation of the CO formed during formic acid electrooxidation. The peak indicates that the Pt surface is roughly 90% saturated with CO. In contrast, with palladium, no peaks are seen in the CO region. Thus, it appears

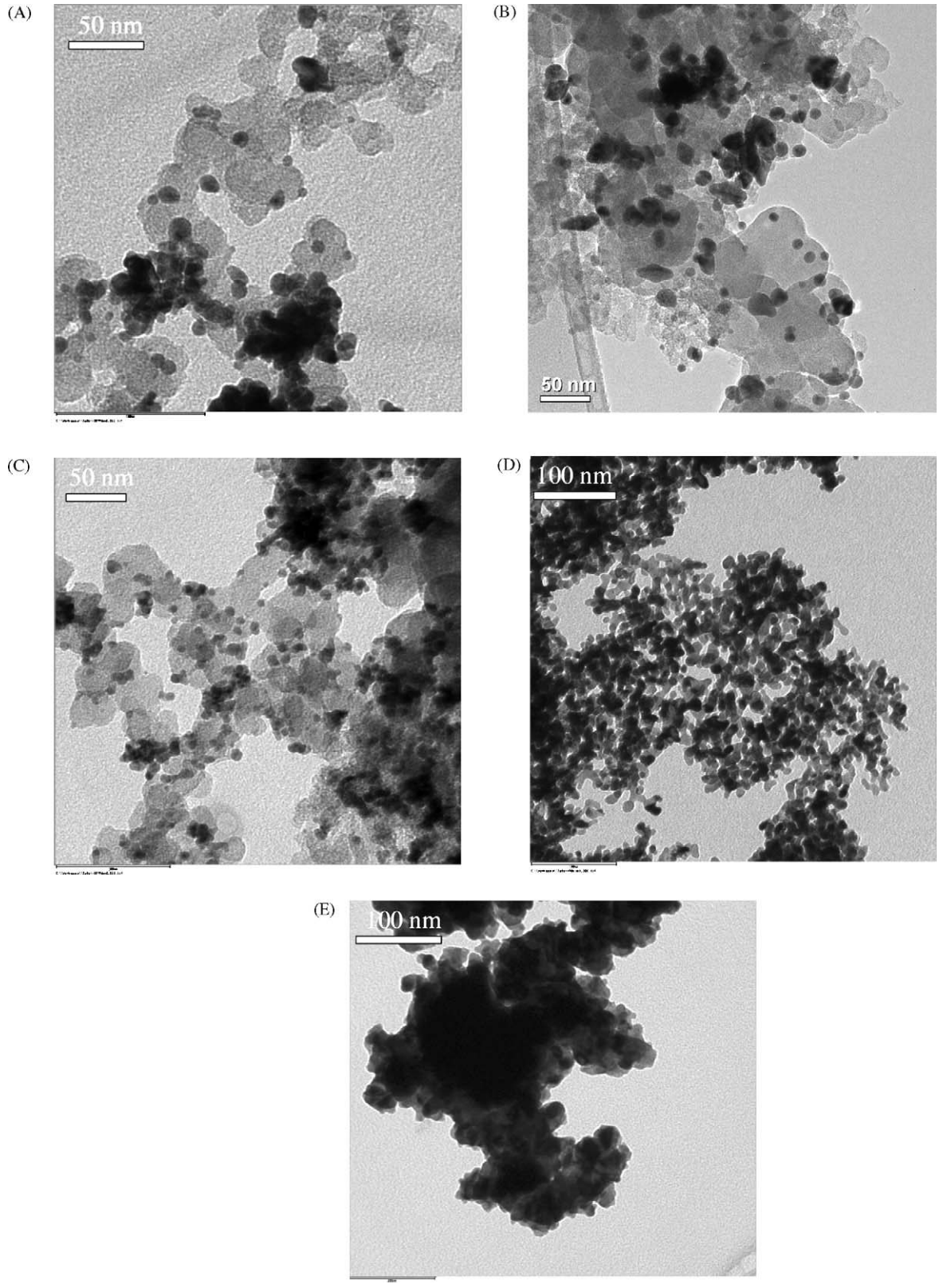

Fig. 1. TEM images of: (A) 20 wt% Pd on carbon; (B) 20 wt% PdAu on carbon; (C) 40 wt% Pd on carbon; (D) Pd black from Sigma–Aldrich ($50\,m^2\,g^{-1}$); (E) Pd black from Alfa Aesar ($20\,m^2\,g^{-1}$).

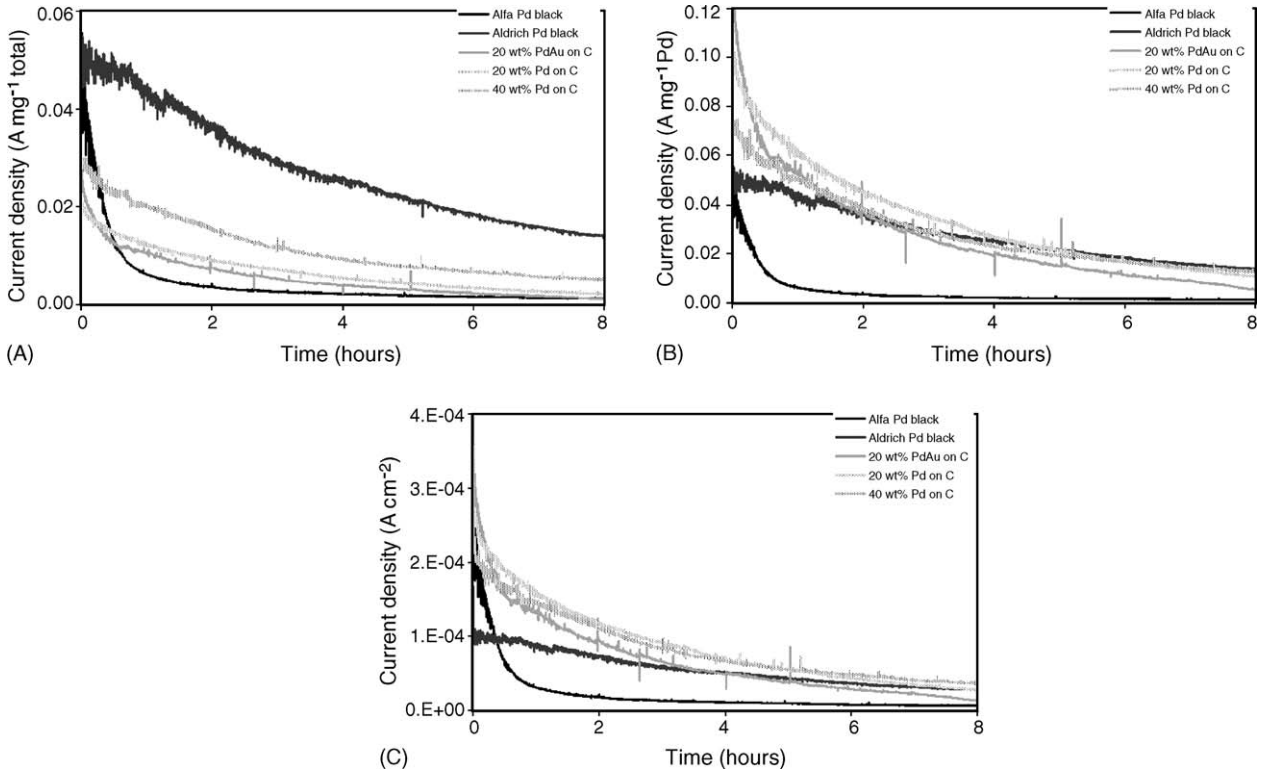

Fig. 2. Chronoamperometric activity of Pd catalysts at 0.3 V vs. RHE (stepping from open cell) in 5 M HCOOH/0.1 M H_2SO_4 exposed to air. Current densities are based on: (A) total catalyst weight; (B) Pd weight; (C) active catalyst surface area.

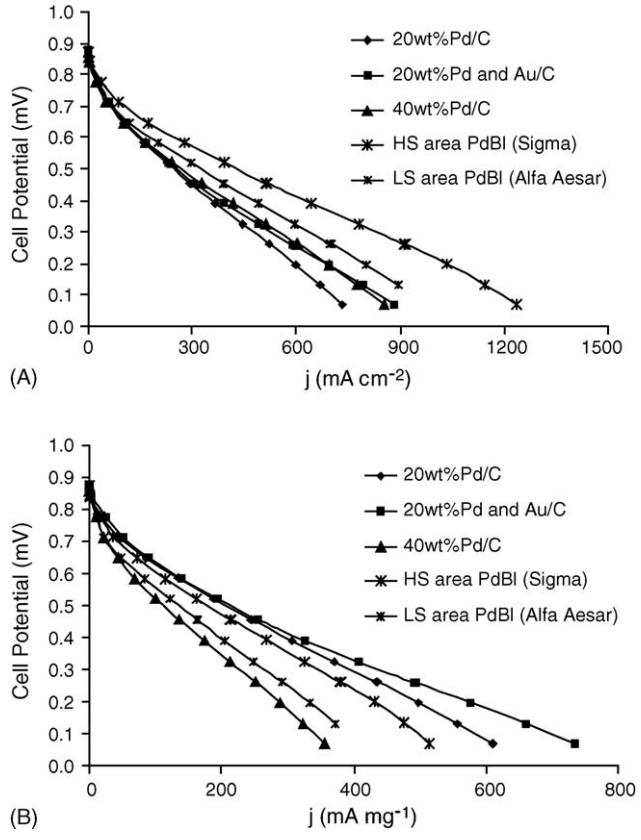

Fig. 3. *V–I* plot with current density on a: (A) per membrane surface area basis and (B) per total catalyst weight basis of direct formic acid fuel cell with various Pd anode catalysts operating in dry air at 30 °C with 5 M formic acid.

that there is no buildup of CO on the catalyst during formic acid electrooxidation on palladium.

4. Discussion

Traditional Pt-based catalysts are thought to follow a dual pathway mechanism [8,10,11]. In one pathway, formic acid is oxidized directly to CO_2:

$$Pt + HCOOH \rightarrow X \rightarrow Pt + CO_2 + 2H^+ + 2e^- \quad (1)$$

In the other pathway, formic acid is oxidized to CO that must then be removed from the surface by activating water:

$$Pt + HCOOH \rightarrow X \rightarrow Pt\text{–}CO + H_2O \quad (2)$$

$$Pt + H_2O \rightarrow Pt\text{–}OH + H^+ + e^- \quad (3)$$

$$Pt\text{–}CO + Pt\text{–}OH \rightarrow 2Pt + CO_2 + H^+ + e^- \quad (4)$$

While the net reaction of the two different pathways is the same, the water activation reaction (3) is difficult. CO can therefore remain on the surface for comparatively long periods of time occupying active catalyst sites and reducing overall activity. By comparison, Pd is thought to proceed primarily via a direct pathway analogous to reaction (1) [8]. Fig. 6 shows that little or no CO builds up on the surface during formic acid electrooxidation on palladium. The absence of CO poisoning means that the activity of Pd catalysts can be much higher than that of platinum. In comparing results from this study with previous results for platinum-based catalysts in formic acid fuel cells [1,2], the performance characteristics of palladium catalysts are superior.

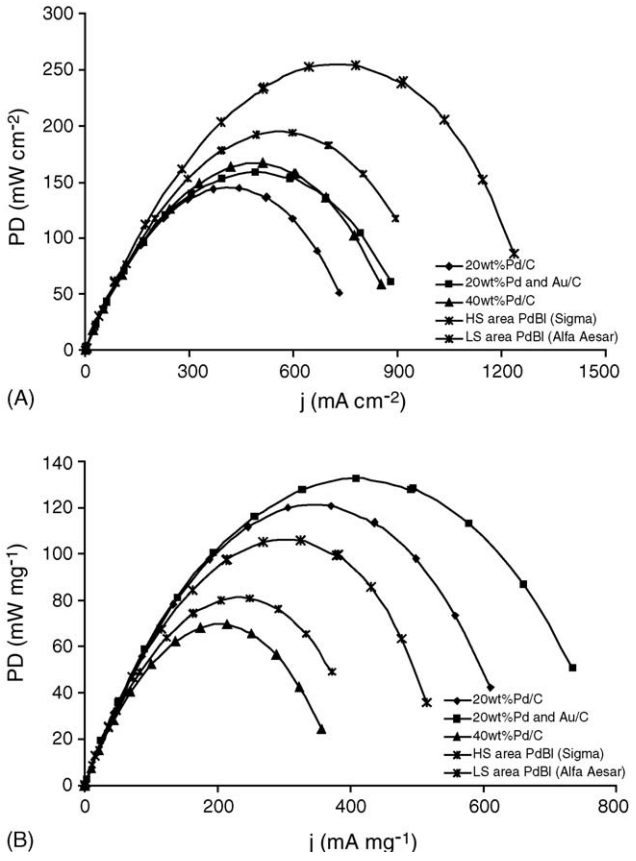

Fig. 4. Power density plots on a: (A) per membrane surface area basis and (B) per total catalyst weight basis of direct formic acid fuel cell with various Pd anode catalysts operating in dry air at 30 °C with 5 M formic acid.

The commercial Pd blacks demonstrate some interesting performance characteristics. The high surface area Pd black from Sigma–Aldrich outperforms the low surface area Pd black from Alfa Aesar even when adjusting for the exposed surface area and this performance difference is quiet large. This suggests either a contamination of the Alfa Pd black during the production process or there is a particle size/morphology effect of the palladium. Fig. 1 shows that the two Pd blacks have quite different structures as well as particle sizes. A size effect is perhaps

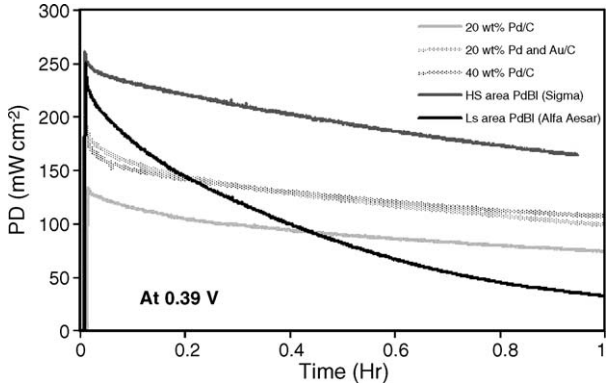

Fig. 5. Direct formic acid fuel cell life test with various Pd anode catalysts operating in dry air at 30 °C with 5 M formic acid.

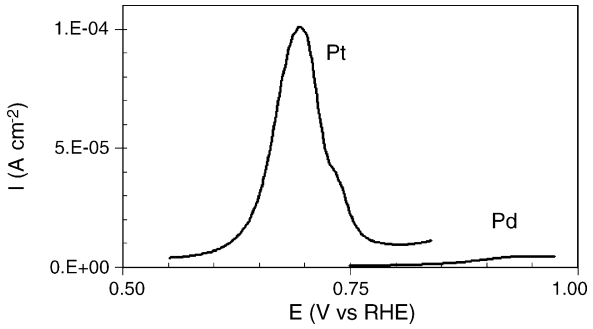

Fig. 6. Quantification of the CO buildup on Pt Black (Johnson-Matthey) and Pd Black (Sigma–Aldrich) after oxidation for 1 h in 5 M HPLC grade formic acid and 0.5 M H_2SO_4 at 0.3 V vs. RHE. After oxidation, the cell was flushed with 0.1 M H_2SO_4 while holding the working electrode at 0.3 V vs. RHE to prevent loss of surface CO. This figure shows CO stripping in the first CV scan.

the reason for Capon and Parsons [8] observation of low activity of formic acid oxidation on Pd foils.

It is interesting to note that the carbon-supported catalysts deactivate at similar rates as the Aldrich Pd black in chronoamperometry and fuel cell constant voltage tests, while the Alfa Pd black deactivates much faster. This again suggests the presence of different morphology or contamination of the Alfa Pd black. In practice, reasonable deactivation rates for the Pd catalysts are acceptable, since the catalyst is readily regenerated by a 1 s pulse at 1.0 V versus RHE every 30 min or so [5,6]. The energy for such a pulse would be stored during fuel cell operation and released every so often to keep the fuel cell running at high activity levels.

In general, the carbon-supported catalysts perform quite well. Their performance tends to be lower than the high surface area Aldrich Pd black on a total catalyst basis, but when comparing on a per Pd weight basis or active surface area basis, the carbon-supported catalysts tend to do as well or better than the unsupported Aldrich Pd black. The more efficient use of Pd in the carbon-supported catalysts means Pd loadings, and thus, overall catalyst expense, can be reduced. However, there is a limited amount of total catalyst (Pd + carbon) that can be loaded onto a fuel cell membrane, typically 6–8 mg cm^{-2} of membrane surface area for these carbon-supported catalysts. Therefore, the total amount of Pd on the membrane can often be much less than for an unsupported catalyst offsetting the improved efficiency of use of Pd. In addition, for a given amount of Pd, the catalyst layer will be thicker for a carbon-supported catalyst potentially causing mass transfer problems at higher current densities. As Table 1 shows, the dispersions of the carbon-supported catalysts are quite low. Much potential for improvement of the carbon-supported catalysts exists through the addition of promoters or better nanoparticle preparation methods to prevent particle agglomeration and reduce nanoparticle size. Just a three-fold improvement in catalyst dispersion could make carbon-supported catalysts superior to the unsupported Aldrich Pd black.

Comparing the TEM images in Fig. 1 with the data in Table 1, one would expect the 20 wt% PdAu on carbon catalyst to have a slightly higher active surface area than the 20 wt% Pd on car-

bon catalyst due to the lesser degree of agglomeration of the PdAu catalyst. However, the opposite is observed. The PdAu catalyst has a lower dispersion and active surface area, yet Figs. 2–4 demonstrate that the PdAu catalyst has the higher activity. Clearly, the addition of gold to the catalyst is aiding the electrooxidation of formic acid in some manner through either electronic modification of the catalyst, a two-body effect or catalytic activity of gold towards poisons/formic acid. Previous studies have suggested that gold and palladium together would be beneficial for the oxidation of formic acid [5,7] and the fuel cell results in Figs. 3 and 4 confirm this electrochemical data.

Comparing the data for 20 and 40 wt% Pd on carbon in Fig. 1 and Table 1 also suggests that higher loadings of Pd on carbon will lead to more agglomeration of nanoparticles and hence lower utilization of exposed palladium atoms. In order to use higher loadings of Pd dispersed on carbon, promoters or different preparation methods may be beneficial to reduce Pd nanoparticle size and agglomeration.

5. Conclusion

This study investigated several unsupported and supported Pd catalysts and confirmed our previous studies that palladium-based catalysts show promise for use in direct formic acid fuel cells. It was found that high surface area Pd catalysts produce excellent results in a fuel cell while a low surface area Pd black showed rapid deactivation and much lower activity, possibly due to a particle size effect. Carbon-supported Pd catalysts demonstrate good activity along with the potential for more efficient Pd metal utilization and lower metal loadings. Addition of gold to carbon-supported Pd improves catalyst performance, suggesting that activity of Pd-based catalysts can be further improved. Eventually, carbon-supported catalysts may even be able to outperform unsupported Pd blacks overall. Using Pd-based catalysts allows for remarkable maximum power densities in a fuel cell of 150–260 mW cm^{-2}, approaching hydrogen fuel cell performances.

Acknowledgments

This work is supported by the Defense Advanced Research Projects Agency under U.S. Air Force Grant F33615-01-C-2172 and by a National Science Foundation Graduate Research Fellowship. Any opinions, findings and conclusions or recommendations expressed in this publication are those of the authors and do not necessarily reflect the views of the Defense Advanced Research Projects Agency, the U.S. Air Force, or the National Science Foundation.

References

[1] C. Rice, S. Ha, R.I. Masel, P. Waszczuk, A. Wieckowski, T. Barnard, Direct formic acid fuel cells, J. Power Sources 111 (1) (2002) 83–89.
[2] C. Rice, S. Ha, R.I. Masel, A. Wieckowski, Catalysts for direct formic acid fuel cells, J. Power Sources 115 (2) (2003) 229–235.
[3] Y.W. Rhee, S.Y. Ha, R.I. Masel, Crossover of formic acid through Nafion((R)) membranes, J. Power Sources 117 (1–2) (2003) 35–38.
[4] P. Waszczuk, T.M. Barnard, C. Rice, R.I. Masel, A. Wieckowski, A nanoparticle catalyst with superior activity for electrooxidation of formic acid (vol. 4, p. 599, 2002), Electrochem. Commun. 4 (9) (2002) 732.
[5] R. Larsen, J. Zakzeski, Y. Zhu, R.I. Masel, Unexpected activity of palladium nanoparticle catalysts in formic acid fuel cells, Electrochem. Solid State Lett. 8 (6) (2005) A291–A293.
[6] S. Ha, R. Larsen, Y. Zhu, R.I. Masel, Direct formic acid fuel cells with 600 A/cm^2 at 0.4 V and 22 °C, Fuel Cells 4 (4) (2004) 337–343.
[7] M. Baldauf, D.M. Kolb, Formic acid oxidation on ultrathin Pd films on Au($h\,k\,l$) and Pt($h\,k\,l$) electrodes, J. Phys. Chem. 100 (27) (1996) 11375–11381.
[8] D. Capon, R. Parsons, The oxidation of formic acid on noble metal electrodes: a comparison of the behaviour of pure electrodes, Electroanal. Chem. Interfacial Electrochem. 44 (1973) 239–254.
[9] S. Biella, F. Porta, L. Prati, M. Rossi, Surfactant-protected gold particles: new challenge for gold-on-carbon catalysts, Catal. Lett. 90 (1–2) (2003) 23–29.
[10] A. Wieckowski, J. Sobkowski, Comparative study of adsorption and oxidation of formic acid and methanol on platinized electrodes in acidic solution, J. Electroanal. Chem. 63 (1975) 365–377.
[11] R. Parsons, T. Vandernoot, The oxidation of small organic-molecules—a survey of recent fuel-cell related research, J. Electroanal. Chem. 257 (1–2) (1988) 9–45.